

# **On the Numerical Simulation of Non-smooth, Resonant Vibrations of Delaminated Structures**

Ingolf Müller, Peter Vielsack, Karl Schweizerhof  
Universität Karlsruhe (TH), Institut für Mechanik

Institut für Mechanik  
Kaiserstr. 12, Geb. 20.30  
76128 Karlsruhe  
Tel.: +49 (0) 721/ 608-2071  
Fax: +49 (0) 721/ 608-7990  
E-Mail: ifm@uni-karlsruhe.de  
[www.ifm.uni-karlsruhe.de](http://www.ifm.uni-karlsruhe.de)

# On the Numerical Simulation of Non-smooth, Resonant Vibrations of Delaminated Structures

Ingolf Müller, Peter Vielsack and Karl Schweizerhof

Institut für Mechanik  
Universität Karlsruhe (TH)  
D-76131 Karlsruhe, Germany  
e-mail: mechanik@ifm.uni-karlsruhe.de

**Abstract.** Oscillation properties of delaminated structures are governed by dissipative impact-like contacts in the debonded region. The contribution focuses on the numerical simulation of this special type of contact. A robust and efficient contact strategy is presented mainly based on the theory of sudden impacts embedded in Finite Element methods.

## 1 Introduction

Composite laminates are being increasingly used as primary structural components in various engineering fields due to their inherently high specific mechanical properties. Correspondingly, a major interest lies in non-destructive testing of the structural integrity, particularly in relation to the occurrence of delaminations between adjacent plies as one of the most common failure modes in composite laminates.

The need for quantitative global damage detection methods has led to the development and continued research into vibration based methods [1]. Investigations of the nonlinear vibrational response are promising for localization and to quantify the size of the delamination on a global basis. The nonlinearity arises from a local contact phenomena, the clapping mechanism. The delaminated layer and the remaining part of a sandwich structure periodically strike against one another during the oscillation [2]. This dynamic contact-impact problem has as the simplest approximation two pendulums which are simultaneously excited by harmonic base excitation [2], [3]. Depending on the frequency and amplitude of excitation, a cascade of bifurcations with intermittent windows of irregular motions and different numbers of impacts during one excitation period can occur [2]. The essential point in this scenario is its dependency on the amount of energy dissipation at each impact [4].

In the following, a more realistic situation will be considered. The delaminated sandwich beam consists of two separated laminae with different cross sections. First, experiments are performed to provide a realistic reference for the oscillation behavior dominated by the continuously evolving lateral contact. Second, a mechanical model for this continuous system is proposed based on the discretization into a system with multi degrees of freedom derived by Finite Element methods. Now, the fundamental challenge consists in the reliable capturing of the periodically appearing impact-like dynamic contacts within the stationary state of motion. It will be shown that standard procedures for contact modeling in FE methods as given by the penalty formulation are associated with a distinct sensitivity of the computed solution in regard to the chosen regularization parameters. In an effort to overcome these difficulties, a promising alternative approach of remarkable robustness is addressed for description of impact-like contacts which is mainly based on the theory of sudden impacts involving contact dissipation.

## 2 Experimental Investigations

The mechanical system under consideration is depicted in figure 1 [a]. It consists of two laminae, whose shapes distinctly deflect from an ideal straight line in the static stress-free state. Both laminae

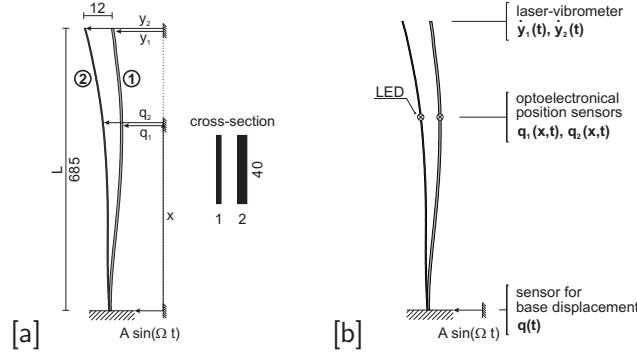


**Fig. 1:** Mechanical system: [a] geometry, [b] sensors.

of length  $685\text{mm}$  are clamped at the lower ends. The upper ends are free. The maximum width of the gap at the upper ends is  $12\text{mm}$  at rest. Both laminae are made from aluminium. The cross-sections are  $2 \times 40\text{mm}$  (thick lamina (1)) and  $1 \times 40\text{mm}$  (thin lamina (2)), respectively. The displacements  $q_1(x, t)$  and  $q_2(x, t)$  at the distance  $x$  along the vertical at time  $t$  are absolute quantities. The base excitation  $A \sin(\Omega t)$  is harmonic with amplitude  $A$  and driving angular frequency  $\Omega$ . In the following, the amplitude  $A = 2.5\text{mm}$  will be kept constant and only the frequency  $\Omega = 2\pi f$  will be changed. To characterize the properties of the oscillations several sensors are used. Two optoelectronic position sensors give the distance of two corresponding LEDs to a vertical reference. In this way, the initial shape  $q_{1,0}(x)$  and  $q_{2,0}(x)$  of both laminae and the displacements  $y_1(t) = q_1(L, t)$  and  $y_2(t) = q_2(L, t)$  at the top will be monitored. For some selected excitation frequencies the deflection curves  $q_1(x, t)$  and  $q_2(x, t)$  during the oscillation are captured. Additionally, a laser vibrometer measures the velocity  $\dot{y}_1(t)$  and  $\dot{y}_2(t)$  at the upper end of both laminae. A position sensor at the lower end controls the amplitude of excitation  $A$ . Two stationary time-displacement response curves with different

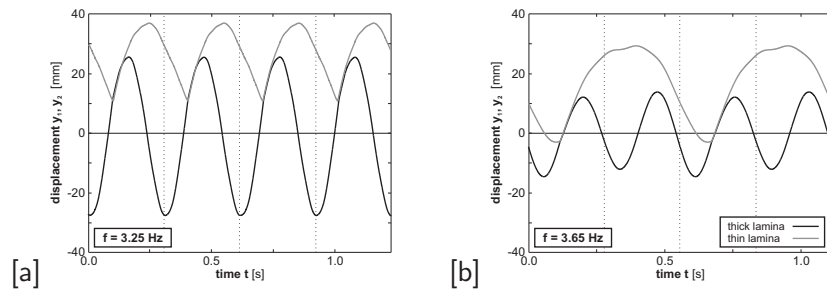


**Fig. 2:** Time-displacement curves for different excitation frequencies and constant amplitudes (experiment).

frequencies of excitation (the used values  $f = \{3.25\text{Hz}, 3.65\text{Hz}\}$ ) are chosen from a frequency range of  $0.5\text{Hz} \leq f \leq 4.0\text{Hz}$ , where the lowest natural frequencies of both laminae can be found. The selected frequencies involve a strong contact interaction of both parts, due to the coupling of both subsystems.

The value  $f = 3.25\text{Hz}$  lies in the vicinity of the resonance of the subsystem with coordinate  $y_1$  (thick lamina). As can be seen in figure 2 [a], the thin lamina is hit by the thick one. In contrast, an excitation frequency  $f = 3.65\text{Hz}$  lies within a window of bifurcated oscillations. Period doubling occurs in such a way that one contact in two excitation periods can be found.

To explore the phenomenon of a continuously evolving contact line during the oscillation in more



**Fig. 3:** Operation deflection shape during one excitation period  $T$ ,  $f = 3.25\text{Hz}$  (experiment).

detail, Figure 3 depicts several states of the deflection shape during one period of excitation  $T$ . In fact, the contact duration is not constant for specific points along the beam axis. Despite this fact, in the following, the only considered point at the tip of the beams is supposed to be representative for the total motion.

As can be seen (Fig. 2), the time interval of contact during one period of excitation is relatively large. Such a phase of common motion of both laminae is only possible if the initial impact, which initiates the contact phase, is highly dissipative. Otherwise, both laminae would separate immediately.

In Figure 4 the velocities  $\dot{y}_1(t)$  and  $\dot{y}_2(t)$  of both laminae within two periods of excitation with  $f = 3.25\text{Hz}$  are captured. The discontinuity (jump) in the velocities at the beginning of contact

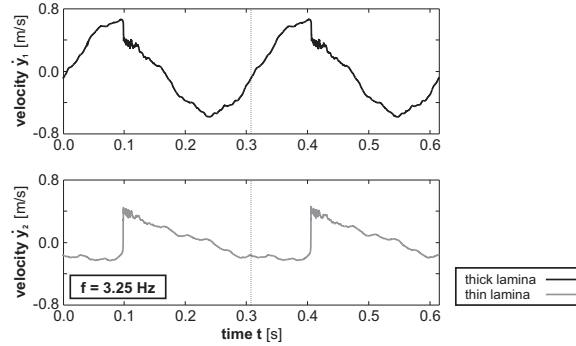


**Fig. 4:** Impact-dominated velocities of both laminae at the free ends in the delamination problem (experiment).

at the considered point is clearly visible. It is evident that this phenomenon can be described by classical impact theory. This theory links the relative velocity  $\dot{Q}(t^{(c)-}) = \dot{q}_u(t^{(c)-}) - \dot{q}_v(t^{(c)-})$  of the impacting masses  $m_u$ ,  $m_v$  before contact and the relative velocity  $\dot{Q}(t^{(c)+}) = \dot{q}_u(t^{(c)+}) - \dot{q}_v(t^{(c)+})$  after contact by a coefficient of restitution  $e$

$$\dot{Q}(t^{(c)+}) = -e\dot{Q}(t^{(c)-}). \quad (1)$$

The corresponding coefficient of restitution  $0 \leq e \leq 1$  depends on the amount of energy dissipation at contact time  $t^{(c)}$ . To find this coefficient, the velocities  $\dot{y}_1(t^{(c)-})$ ,  $\dot{y}_2(t^{(c)-})$  before impacting at the tip and  $\dot{y}_1(t^{(c)+})$ ,  $\dot{y}_2(t^{(c)+})$  after the impact are taken from the experiment. The ratio of masses is approximately given by the ratio of cross-sections as  $m_1/m_2 = 1/2$ . Within the scope of the experimentally gained data, the well-known formulas of NEWTON's impact law reveal a range of  $0 \leq e \leq 0.1$  for the restitution coefficient. This result confirms the large contact damping values found for lateral impacts on beams.

### 3 Computation by Finite Element Methods

For the numerical calculation, the one-dimensional continuum problem is transformed into two multi-DOF systems by FE methods. Both laminae are discretized by the same number of EULER-BERNOULLI beam elements. This leads to the semi-discrete equations of motion as two linear systems with  $2n$  DOF

$$\begin{aligned} \mathbf{M}_1 \ddot{\mathbf{q}}_1(t) + \mathbf{C}_1 \dot{\mathbf{q}}_1(t) + \mathbf{K}_1 \mathbf{q}_1(t) &= \mathbf{f}_1(t) \\ \mathbf{M}_2 \ddot{\mathbf{q}}_2(t) + \mathbf{C}_2 \dot{\mathbf{q}}_2(t) + \mathbf{K}_2 \mathbf{q}_2(t) &= \mathbf{f}_2(t) . \end{aligned} \quad (2)$$

The generalized coordinates given in eq. (2) can be subdivided into translatory and rotational DOFs leading to the displacements  $u$  and the rotations  $\varphi$

$$\mathbf{q}_i = \left[ u_{i,1}, \varphi_{i,1}, \dots, u_{i,n/2}, \varphi_{i,n/2} \right]^T \quad \text{with } y_i = u_{i,n/2} \quad i = 1(1)2 . \quad (3)$$

A prescribed displacement as a harmonic base excitation is applied to the lowest node of each subsystem. Additionally, a clamped support is assumed at these nodes. Coupling of both subsystems, represented by the two sets of equations (2), occurs because of several lateral contact events along the longitudinal axis of the beams. This fact causes the strong nonlinearity of the problem. The continuous evolution of the contact line must be separated into several node-to-node contacts of opposite nodes. During the oscillation the succession of contact points and the corresponding time when contacts occur are unknown *a priori*. These are typical features of a non-smooth dynamic system.

Dealing with non-smooth dynamic systems within FE methods, two fundamental challenges appear, namely to find an appropriate problem-oriented procedure of time integration and to capture the respective contact situation within the numerical contact formulation. The first one is connected with the accuracy of detecting the switching times (contact times) of the non-smooth system to be integrated [5]. In general, in view of the numerical time integration with a certain discrete time step  $\Delta t$  only a limited degree of accuracy can be achieved in regard to determine the contact times. This leads to permanent numerical disturbances in the course of the motion. The undisturbed problem is orbitally stable as long as these disturbances remain below a critical limit. Thus, a sufficiently small time step  $\Delta t$  is needed for an orbital stable solution. The present contribution will not focus to the problem of an appropriate time integration. Here, the standard NEWMARK scheme ( $2\alpha_N = \beta_N = 1/2$ ) is adopted as the number of DOFs is rather small though the central difference scheme may also be appropriate. Thus, mainly the second problem of the contact formulation will be discussed in the following.

#### 3.1 Contact Description via Penalty Method

Standard procedures in FE methods for contact modeling are the LAGRANGE method, the Augmented-LAGRANGE method and the penalty method. The main problem of all methods is the inclusion of the strongly dissipative character of the dynamic contact. Applications of the first two procedures are not known in this field. The classical penalty method, however, can be extended by introducing penalty damping in addition to the penalty stiffness. Thus, this procedure requires the choice of two penalty parameters, which essentially have no physically specifiable quantity [6]. Moreover, these parameters are mutually dependent on the time step of integration [3]. A parameter estimation is only possible by comparing numerical results with an experimental reference for stationary oscillations [4].

Suppose that the system contains  $n_N$  possible pairs of contact nodes, then the actual state of contact is given by a set of indices  $\mathcal{M}_C$  from all  $n_C$  contact points, which are closed at present time  $t$ . In the

considered case of a time-discrete system with constant time steps  $\Delta t$ , a contact event is captured by the condition

$$g_{N,k_C} = u_{2,k_C} - u_{1,k_C} \leq 0, \quad \forall k_C \in \mathcal{M}_C. \quad (4)$$

Then the overall state of contact at the actual time  $t$  reads

$$\begin{aligned} \mathcal{M}_N &= \{1(1)n_N\} \\ \mathcal{M}_C(t) &= \{k_C \in \mathcal{M}_N \mid g_{N,k_C} \leq 0\}. \end{aligned} \quad (5)$$

After each time step  $\Delta t$  the contact condition is checked. For all contact points contained in the index set  $\mathcal{M}_C$  penalty stiffness  $c_k$  and penalty damper  $c_d$  must be applied. As a benchmark problem

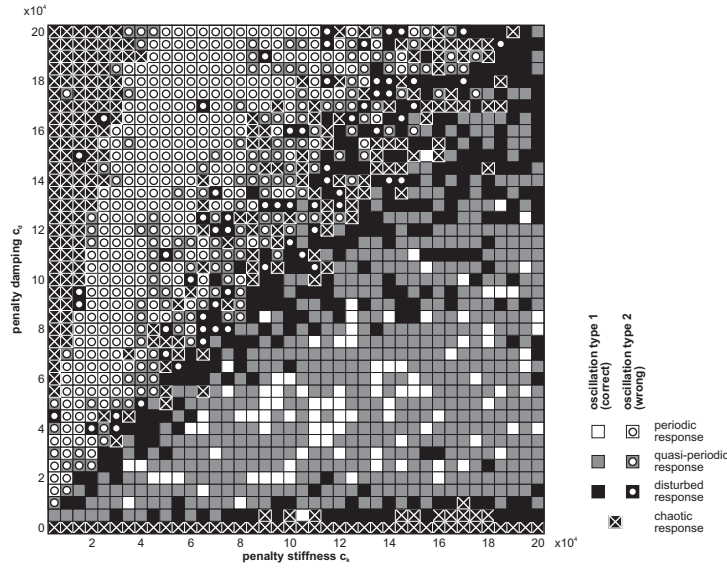


**Fig. 5:** Parametric plane for sets of penalty parameters  $c_K$ ,  $c_D$ .

the time response of the experiment with excitation frequency  $f = 3.25\text{Hz}$  (Fig. 2) is considered. Figure 5 contains a parametric plane that separates regions containing the correct type of solution from regions of distorted types of motion arising from an incorrect set of parameters. For this purpose, the numerical results computed for certain sets of parameters  $c_K$  and  $c_D$  have been categorized in comparison to the experimental results. Figure 5 reveals a distinct parameter sensitivity of the numerical solution in regard to the regularization parameters. All sets of parameters taken from an upper left triangle in the parameter space (see Fig. 5) are associated with an incorrect numerical solution - a bifurcated oscillation. In the considered parameter range a qualitatively correct result is obtained only in a few cases (Fig. 5: white bricks). Without further information about the expected motion, a decision is not possible, whether the chosen set of penalty parameters is correct or not. Furthermore, treating another type of oscillation, a different calibration of the penalty parameters  $c_K$ ,  $c_D$  is required, which have further to be adjusted to the time step of the integration. Due to these facts, the described penalty regularization can not be considered as an appropriate contact description for the treated type of contact.

### 3.2 Contact Description via an Impact Formulation

Sudden impacts accompanied by strong energy dissipation can be modeled by the classical theory of impact in which the velocities during a contact event are controlled by a law of impact, e.g. NEWTON's impact law. This procedure, which has been proven in the field of rigid body dynamics,

can be adopted for description of dissipative contact within the Finite Element methods. Applying an impact law, a sudden change of the velocities of the contact nodes within a vanishing time interval is assumed. At each pair of contact nodes the law of impact must be applied.

In contrast to applying a law of impact with vanishing contact duration, the penalty method supposes a phase of permanent contact with a minimal duration of one time step  $\Delta t$  for each contact event. Thus, a partial state of permanent contact is included herein. As a main advantage for computation, this regularization allows a description of permanent contact while the number of DOFs is kept unaltered in comparison to the freely vibrating system.

In the following, the two methods are connected in a way that permits both a sudden impact and a motion in permanent contact. Therefore, the law of impact is employed to capture the impact-like contact phenomena showing a sudden change of the velocities as well as to observe energy dissipation during contact. Contact stiffness is only detached from the penalty method. In the case of permanent contact, this stiffness is employed. Thus, two parameters are required (coefficient of restitution  $e$ , contact stiffness  $c_K$ ), whereas the range of the main parameter  $e$  can be determined by experiments (see fig. 4). However, since contact dissipation is solely captured by the law of impact, the two parameters are almost independent from one another, allowing an almost independent choice for  $c_K$ . This is an additional advantage compared to the classical penalty method.

The system is governed by three partial states in motion, namely separated motion, sudden impact and permanent contact. Again, the actual state of contact at present time  $t$  can be observed by several sets of indices. For this purpose, eq. 5 must be extended to capture all possible cases.

$$\begin{aligned}
\mathcal{M}_N &= \{1(1)n_N\} \\
\mathcal{M}_C &= \{k_C \in \mathcal{M}_N \mid g_{N,k_C} \leq 0\} \\
\mathcal{M}_M &= \{k_M \in \mathcal{M}_C \mid \dot{g}_{N,k_M} \geq \gamma \wedge (k_M \notin \mathcal{M}_{P0}(t_{j-1}) \vee k_M \notin \mathcal{M}_{PP}(t_{j-1}))\} \\
\mathcal{M}_{P0} &= \{k_{P0} \in \mathcal{M}_C \mid \dot{g}_{N,k_{P0}} < \gamma \wedge k_{P0} \notin \mathcal{M}_{PP}(t_{j-1})\} \\
\mathcal{M}_{PP} &= \{k_{PP} \in \mathcal{M}_C \mid k_{PP} \in \mathcal{M}_{P0}(t_{j-1}) \vee k_{PP} \in \mathcal{M}_{PP}(t_{j-1})\} \\
\mathcal{M}_N &: \text{possible contact points } (n_N \text{ elements}) \\
\mathcal{M}_C &: \text{actually closed contact points } (n_C \text{ elements}) \\
\text{with } \mathcal{M}_M &: \text{sudden impact with immediate separation } (n_M \text{ elements}) \\
\mathcal{M}_{P0} &: \text{beginning of permanent contact } (n_{P0} \text{ elements}) \\
\mathcal{M}_{PP} &: \text{persistent permanent contact } (n_{PP} \text{ elements})
\end{aligned} \tag{6}$$

The condition for the occurrence of a contact event  $g_{N,k_C} \leq 0$  can be kept unmodified in relation to eq. (4). Therefore, the law of impact

$$\begin{aligned}
\dot{\mathbf{u}}_1^{(t_j)}(t_j^+) &= \dot{\mathbf{u}}_1^{(t_j)}(t_j^-) + (\mathbf{I} + \mathbf{e}^{(t_j)}) \mathbf{M}_2^{(t_j)} (\mathbf{M}_1^{(t_j)} + \mathbf{M}_2^{(t_j)})^{-1} \dot{\mathbf{g}}_N^{(t_j)}(t_j^-) \\
\dot{\mathbf{u}}_2^{(t_j)}(t_j^+) &= \dot{\mathbf{u}}_2^{(t_j)}(t_j^-) - (\mathbf{I} + \mathbf{e}^{(t_j)}) \mathbf{M}_1^{(t_j)} (\mathbf{M}_1^{(t_j)} + \mathbf{M}_2^{(t_j)})^{-1} \dot{\mathbf{g}}_N^{(t_j)}(t_j^-) \\
\text{with } \mathbf{M}_i^{(t_j)} &= \text{diag}([\bar{m}_{i,kk}]) \quad i = 1(1)2, \forall k \in \mathcal{M}_C(t_j) \vee \mathcal{M}_{P0}(t_j) \\
\mathbf{e}^{(t_j)} &= \text{diag}([e_k])
\end{aligned} \tag{7}$$

must be applied on all pairs of contact nodes contained in the sets of indices  $\mathcal{M}_M$ ,  $\mathcal{M}_{P0}$ . Herein  $\bar{m}_{i,kk}$  denotes the masses affecting the impacting nodes at time  $t^{(j)}$ , which can be estimated from the corresponding translatory DOFs in the diagonalized mass matrix. Furthermore, the diagonal matrix  $\mathbf{e}^{(t_j)}$  contains the coefficients of restitution  $e_k$ . In the following, the restitution coefficient is assumed to be constant for all pairs of contact nodes. Then, only one parameter  $e$  is needed, which is known from the preceding experimental investigation.

A sudden impact marks the beginning of each contact event. In the case of a vanishing translatory, relative velocity  $\dot{g}_N = 0$ , checked at each pair of contact nodes contained in  $\mathcal{M}_c$ , a partial state of permanent contact follows for these contact nodes. For all non-vanishing coefficients of restitution  $e$ ,

this switching condition can lead to a sequence of numerous impacts [7]. To avoid these phenomena, a small threshold  $\gamma$  for the relative velocity is introduced to assign the beginning of motion in permanent contact. Therefore, the weak inequality

$$\dot{g}_{N,k_{P0}} = \dot{u}_{2,k_{P0}} - \dot{u}_{1,k_{P0}} < \gamma, \quad \forall k_{P0} \in \mathcal{M}_{P0}, \quad \gamma \ll 1 \quad (8)$$

allows the decision on whether a state of permanent contact follows on impact or not. In the first case, the penalty stiffness  $c_K$  is added at the corresponding contact nodes indicated by the set of index  $\mathcal{M}_{P0}$ . Contact stiffness  $c_K$  for the corresponding pair of contact nodes remains in the system as long as the separation condition ( $g_{N,k} = u_{2,k} - u_{1,k} > 0, k \in \mathcal{M}_{PP}$ ) is not satisfied. In the following, computations are presented for the two different types of oscillation whose corresponding experimental results are given in Fig. 2. According to the experimental results, the coefficient of

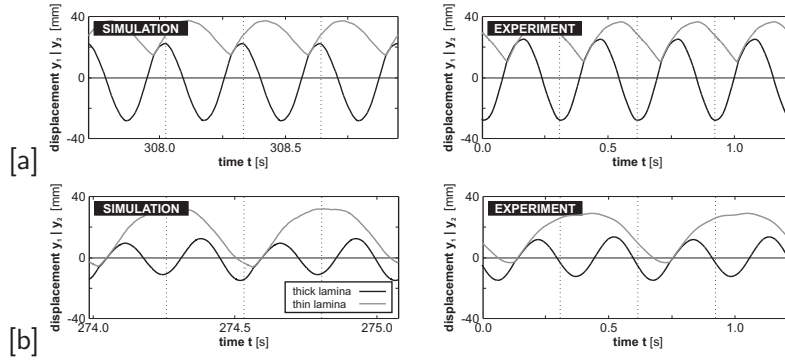


**Fig. 6:** Time-displacement diagram for the stationary motion of both lamina for the two excitation frequencies: [a]  $f = 3.25\text{Hz}$ , [b]  $f = 3.65\text{Hz}$ .

restitution as the main contact quantity is chosen as  $e = 0.10$ . Two additional numerical parameters have to be chosen: the penalty stiffness  $c_K$  and the threshold  $\gamma$  for permanent contact. Contact stiffness is set as  $c_K = 100$ , which is reasonable in this analysis. The threshold of the relative velocity is chosen in such a way that  $\gamma = 0.0005$  is close to 0.1% of the maximum relative velocity. These values are fixed for all cases considered above.

Considering the time histories (see Fig. 6), in all cases excellent agreement of experimental and numerical results can be noted in relation to both the amplitudes and the shape of oscillation. The main advantages over the classical penalty method are evident from this investigation. First, the main parameter  $e$  is experimentally determinable. The additionally required penalty stiffness  $c_K$  exhibits in this connection a very limited influence on the result. Moreover, the chosen set of parameters is applicable without modification to describe all treated types of motion that exhibit a wide variety. Such behavior cannot be expected from the spring-damper regularization by the pure penalty method.

Furthermore, the described contact formulation shows a remarkable robustness concerning the choice of parameters  $e, c_K$  which can be found from the parametric plane of Figure 7. However, apart from a few exceptions, the basic type of response denoted by one contact event in one excitation period is preserved for all cases considered. When estimating the influence of the two parameters, the restitution coefficient mainly affects the solution in the considered range.

## 4 Conclusions

Forced oscillations of delaminated structures are dominated by continuously evolving impact-like contacts. First, the arising contact phenomena are studied experimentally on a realistic model situation



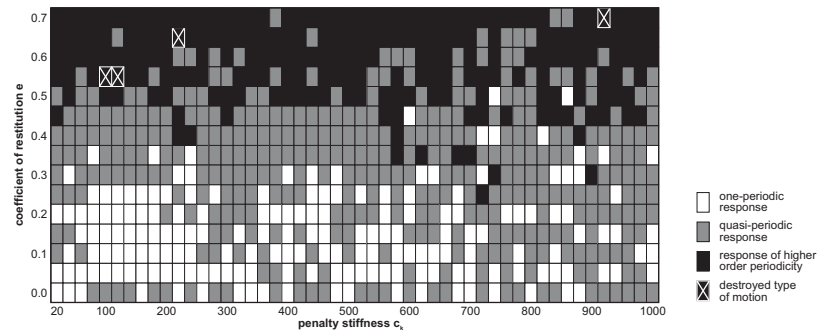


**Fig. 7:** Parametric plane for sets of parameters  $e$ ,  $c_K$ .

for the delamination problem. Depending on the frequency of excitation, a bifurcation scenario occurs. The experiments reveal a distinct amount of energy dissipation during the contact.

Armed with this knowledge, an appropriate contact description for numerical simulation using Finite Element methods is proposed mainly based on the theory of sudden impacts involving contact dissipation. In contrast to the classical penalty method, the main parameter, namely the coefficient of restitution, can be determined easily by experimental means. Computational results document the robustness of the procedure concerning the choice of parameters. In almost all cases considered above, the type of the experimental reference solution was preserved numerically within a large range of parameters. Furthermore, the set of parameters could be kept constant for all of the very different types of motion previously considered.

## References

- [1] Zou L, Tong L, Steven GP (2000) *Journal of Sound & Vibration* 230(2):357–378
- [2] Vielsack P (2002) *Journal of Sound & Vibration* 253(2):347–358
- [3] Müller I, Vielsack P (2003) *Journal of Computational & Applied Mechanics* 4(2):173–186
- [4] Müller I, Konyukhov A, Vielsack P, Schweizerhof K (2005) *Engineering Structures*, 27(2):191–201
- [5] Vielsack P, Hartung A (1999) *ZAMM* 79(6):389–397
- [6] Engleder T, Vielsack P, Schweizerhof K (2002) *Computational Mechanics* 28:162–168
- [7] Valente AX, McClamroch NH, Mezi I (2003) *International Journal of Non-Linear Mechanics* 38(5):677–689